AD-A073 728 ARMY ELECTRONICS RESEARCH AND DEVELOPMENT COMMAND WS--ETC F/G 4/2
THE DYNAMICS OF MATERIAL LAYERS.(U)
JUL 79 W D OHMSTEDE

UNCLASSIFIED ERADCOM/ASL-TR-0036 NL

1 OF 1
AD A073728

END
DATE FILMED
10-79
DDC

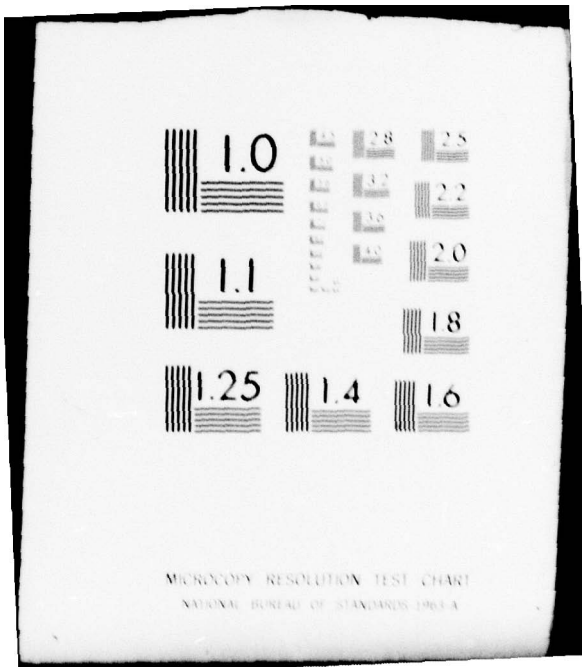
1.0
1.1
1.25
1.4
1.6
2.8
3.2
3.6
4.0
2.5
2.2
2.0
1.8
MICROCOPY RESOLUTION TEST CHART
NATIONAL BUREAU OF STANDARDS 1963 A

ASL-TR-0036

LEVEL II

AD

Reports Control Symbol
OSD 1366

AD A073728

THE DYNAMICS OF MATERIAL LAYERS

July 1979

By

William D. Ohmstede

Approved for public release; distribution unlimited

US Army Electronics Research and Development Command
ATMOSPHERIC SCIENCES LABORATORY
White Sands Missile Range, NM 88002

NOTICES

Disclaimers

The findings in this report are not to be construed as an official Department of the Army position, unless so designated by other authorized documents.

The citation of trade names and names of manufacturers in this report is not to be construed as official Government indorsement or approval of commercial products or services referenced herein.

Disposition

Destory this report when it is no longer needed. Do not return it to the originator.

SECURITY CLASSIFICATION OF THIS PAGE (When Data Entered)

REPORT DOCUMENTATION PAGE

READ INSTRUCTIONS BEFORE COMPLETING FORM

1. REPORT NUMBER: ASL-TR-0036 (14)	2. GOVT ACCESSION NO.: ERADCOM / 3. RECIPIENT'S CATALOG NUMBER: ASL-TR-0036
4. TITLE (and Subtitle): (6) THE DYNAMICS OF MATERIAL LAYERS,	5. TYPE OF REPORT & PERIOD COVERED: (9) R&D Technical Report.
	6. PERFORMING ORG. REPORT NUMBER
7. AUTHOR(s): (10) William D. Ohmstede	8. CONTRACT OR GRANT NUMBER(s)
9. PERFORMING ORGANIZATION NAME AND ADDRESS: Atmospheric Sciences Laboratory, White Sands Missile Range, NM 88002	10. PROGRAM ELEMENT, PROJECT, TASK AREA & WORK UNIT NUMBERS: (6) DA Task 1L161102B53A
11. CONTROLLING OFFICE NAME AND ADDRESS: US Army Electronics Research and Development Command, Adelphi, MD 20783 (11)	12. REPORT DATE: Jul 1979
	13. NUMBER OF PAGES: 49
14. MONITORING AGENCY NAME & ADDRESS (if different from Controlling Office): (12) 54p.	15. SECURITY CLASS. (of this report): UNCLASSIFIED
	15a. DECLASSIFICATION/DOWNGRADING SCHEDULE

16. DISTRIBUTION STATEMENT (of this Report)

Approved for public release; distribution unlimited.

17. DISTRIBUTION STATEMENT (of the abstract entered in Block 20, if different from Report)

18. SUPPLEMENTARY NOTES

19. KEY WORDS (Continue on reverse side if necessary and identify by block number)

Boundary layer modeling
Atmospheric models
Mathematical models
Mesoscale prediction model
Complex terrain

20. ABSTRACT (Continue on reverse side if necessary and identify by block number)

Shallow-fluid equation models have been applied to several Army problem areas, especially those associated with atmospheric transport and diffusion. The objective of this report is to present the development of a system of equations which govern the behavior of material atmospheric layers and which retain the advantages of the shallow-fluid equations but are more generally suitable for atmospheric analysis. The report consists of three major sections. The first section presents a formal derivation of what therein is defined as the "Material Layer Equations." The second section addresses some of the practical

DD FORM 1 JAN 73 1473 EDITION OF 1 NOV 65 IS OBSOLETE

SECURITY CLASSIFICATION OF THIS PAGE (When Data Entered)

20. ABSTRACT (cont)

considerations involved in applications of the material layer equations. Although the presentation of numerical algorithms for specific applications of the material layer equations is beyond the scope of this report, the third section does present elementary examples of how the material layer equations may be specialized to address specific atmospheric analysis problems. It is concluded that the material layer approach is most useful when the matter of concern is the transport and diffusion of material such as from NBC weapons or smoke.

CONTENTS

INTRODUCTION

The Army's requirements for meteorological information are diverse [1]. Over the last several decades, the foremost Army meteorological problem areas have been tube artillery ballistics and chemical/biological warfare/defense. The latter is especially dependent on meteorological information since atmospheric transport/diffusion is an integral part of weapon deployment systems (similar remarks pertain to the deployment of smoke as a battlefield obscurant).

The requirements for meteorological information cannot always be satisfied by one or even several atmospheric observations. The atmosphere may respond to complex terrain in unexpected ways. This problem was manifested by the alleged "sheep" incident at Dugway Proving Ground a decade ago. This situation motivated investigations regarding the numerical modeling of atmospheric flow in association with complex terrain. The primary approach that has been used is based upon the shallow-fluid equations (see Meyers and Dettling [2], Tingle and Bjorklund [3,4], and Dumbauld and Bjorklund [5]). The shallow-fluid equation models have reached the stage of development where they have had operational use in Army test and evaluation activities associated with transport and diffusion problems. On yet another front, a shallow-fluid equation model has been developed [6] with the object of short-term mesoscale predictions for artillery ballistics.

As useful as the shallow-fluid equations might seem for some Army requirements, they may be better suited to the Navy since the equations are far more valid for the hydrosphere than the atmosphere. Acknowledging the utility of the shallow-fluid equations but recognizing their limitations, this report develops the theoretical basis for "atmospheric material layer equations" and discusses the more general utility of this approach to atmospheric problems.

The report consists of three major sections. The first section presents a formal derivation of what herein is defined as the "Material Layer Equations." The second section addresses some of the practical considerations involved in applications of the material layer equations. Although the presentation of numerical algorithms for specific applications of the material layer equations is beyond the scope of this report, the third section does present elementary examples of how the material layer equations may be specialized to address specific atmospheric analysis problems.

MATERIAL LAYERS

The atmosphere is a relatively thin layer of gas clinging to the earth as a consequence of the forces of gravity and friction at the earth's surface. The atmospheric layer is itself internally laminate, consisting of overlapping layers with differing air mass properties. Observers can perceive material layers in the atmosphere when ascending or descending in an aircraft through haze layers. These layers are

especially manifest in industrialized regions where atmospheric pollution is trapped within a material layer which is separated from a superior unpolluted air mass by a stable subsidence inversion.

Formally, a material layer is one which is mass conservative as a consequence of being bounded by material surfaces through which there is no mass transport. A material (or Lagrangian) surface (interface) is one wherein air parcels are confined to two-dimensional motion. The atmosphere does not contain material interfaces such as those which occur between immiscible fluid layers; however, there are hydrostatically stable layers in the atmosphere which commonly behave as the equivalent of immiscible material layers.

The behavior of the atmosphere can be fully understood only if the importance of material layers is adequately recognized. The kinematic, thermodynamic, and weather structure of the atmosphere is intimately related to the dynamics of material layers. One of the greatest breakthroughs in meteorology has been the introduction of frontal and air mass analysis by J. Bjerknes and collaborators [7]. Weather satellite pictures continue to confirm the great foresight of these Norwegian pioneers in describing the properties of air masses (material layers) and associated fronts (material interfaces), and their role in extratropical cyclone development. Frontal inversions are only one example of material interfaces which affect atmospheric behavior. The tropopause, subsidence inversions, and the upper (nonturbulent) portion of surface inversions are additional significant atmospheric material surfaces. The foremost material surface, however, is the air/earth interface which causes major terrain and diabatic effects on atmospheric structure and behavior.

During the last two decades, a "creeping" breakthrough has occurred in meteorology associated with the development and improvement of high-speed digital computers and the concomitant development of numerical models for diagnostic/prognostic analysis of atmospheric structure. Progress in this area has been rapid and the operational primitive-equation model described by Shuman and Hovermale [8] is surely a great achievement. Further progress is assured; the only practical limit is the capacity and capabilities of computers.

Unwittingly, the numerical model fad has, especially in the early phases, tended to push interest in material layers into the background. The bold atmospheric structure associated with material layers was incongruous with demands for smoothness by the elementary numerical models. Fortunately, there is increasing relaxation of this stricture; for example, the primitive-equation model of the National Weather Service [8] recognizes and maintains the troposphere/stratosphere partitioning.

In another area, in the last several decades, interest has developed concerning the existence and nature of hydraulic jumps in the

atmosphere associated with the flow of stratified (material) layers. On the one hand, Freeman [9] and Tepper [10] have suggested that hydraulic jumps associated with traveling gravity waves on subsidence inversions are the long sought explanation for squall lines. On the other hand, Houghton and Kasahara [11] and Long [12] have mathematically investigated the properties of hydraulic jumps associated with stratified flow over barriers.

The shallow-fluid equations, prominent in hydrodynamics and oceanography (see Stoker [13]), are the approach frequently used in the investigation of the flow of stratified fluids. Stoker [14], Kasahara, Isaacson, and Stoker [15], and Turkel [16] have used various forms of the shallow-fluid equations to investigate frontal motion in the atmosphere. Freeman [6], Lavoie [17], and Tingle and Bjorklund [3,4] have reported on numerical shallow-fluid models which are useful for investigating terrain effects on atmospheric flow.

Hydraulic jumps, if only transitory, are a characteristic feature of the shallow-fluid equations. The use of the shallow-fluid equations in the development of numerical models has required intensive investigations of numerical algorithms which are computationally stable and yet accommodate the jump discontinuities. The works of Lax and Wendorf [18] and Sundstrom [19] are significant examples of this effort. Although the subject of hydraulic jumps and their solution has developed into a minor fad, this does not detract from the fact that the introduction of the shallow-fluid equations into atmospheric dynamics has been a major step towards returning material layers to the prominence that they deserve in atmospheric diagnostic/prognostic analysis.

The classical shallow-fluid equations pertain to the flow of immiscible layers of incompressible fluid that are so shallow that the vertical shear structure is essentially irrelevant and the mean velocity in the layer is sufficient to describe the flow. The great power of the shallow-fluid equations is manifest in their strong conservation of mass and energy; however, the classical shallow-fluid equations are only crude approximations when applied to the atmosphere.

MATERIAL LAYER DYNAMICS

The development of the material layer equations begins with a standard set of atmospheric variables. Initially, the coordinate system is a Cartesian conformal projection of a relatively small region of a rotating earth, but a vertical coordinate transformation conforming to the material surfaces alters the basic dynamic equations so as to be consistent with the hypothesis of no mass transport through the bounding material surfaces. Integration of the transformed equations results in the material layer equations.

Basic Meteorological Variables

The independent variables are time (t) and a Cartesian system of space coordinates (x,y,z). The space coordinates correspond with a position vector ($x^i | i = 1,2,3$). Within this report, a superscripted variable denotes a component of a vector. In this case, $x^1 \equiv x$, $x^2 \equiv y$, $x^3 \equiv z$. The coordinate system rotates with the earth such that a space point remains stationary relative to a fixed point on the earth's surface. The vertical coordinate ($x^3 \equiv z$) is proportional to the geopotential (Φ). Thus, z is the geopotential height with the origin at mean sea level. The horizontal coordinates (x,y) correspond with the appropriate Universal Transverse Mercator (UTM) grid. In a local region, the UTM conformal projection has very little distortion so that the mapping scale factor is taken to be unity.

The principal dependent variables are: the thermodynamic state variables, consisting of the pressure (p), temperature (T), density (ρ), and specific humidity (q); and the kinematic variables, consisting of the velocity vector ($u^i | i = 1,2,3$; or u,v,w), the momentum (or mass flux) vector ($m^i | i = 1,2,3,$; sometimes written as m^x, m^y, m^z), and the water flux vector ($n^i | i=1,2,3$; n^x, n^y, n^z). The variables above are taken to be locally averaged variables. Whenever there is turbulence present, additional turbulence terms must be defined. The more important turbulence terms are the turbulent heat flux vector ($\zeta^i | i = 1,2,3$), the turbulent mass flux vector ($\mu^i | i = 1,2,3$), the turbulent water flux vector ($\nu^i | i = 1,2,3$), the Reynolds stress tensor ($\tau^{ij} | i,j = 1,2,3$), and the turbulence pressure (ε). Formal definitions of these and other variables may be found in the Glossary of Symbols. Note here the following relationships.

$$m^i = \rho u^i + \mu^i \tag{1a}$$

$$n^i = q m^i + \nu^i \quad i = 1,2,3 \tag{1b}$$

$$\zeta^i = -\mu^i T \tag{1c}$$

The latter equation arises from the assumption that turbulent pressure fluctuations are negligible.

Basic Equations

The functional basis for this development is a rather standard system of equations for the state and kinematic variables in a turbulent atmosphere. The foremost expression is the equation of state

$$p = \rho R T \tag{2}$$

The remaining expressions are dynamic equations. The simplest is the equation of continuity.

$$\rho_t + m^\alpha_\alpha = 0 \ . \tag{3}$$

The subscripts in this and the following equations denote partial differentiation. For example, ρ_t corresponds with $\partial\rho/\partial t$. Whenever repeated Greek indices occur, the Einstein summation convention is to be used. For example,

$$m^\alpha_\alpha = \partial m^1/\partial x^1 + \partial m^2/\partial x^2 + \partial m^3/\partial x^3 \ . \tag{4}$$

It is common practice for meteorologists to use the shallow atmosphere approximation when deriving the equations of motion for a rotating earth. Phillips [20] has transformed the equations of motion from an inertial reference frame to a spherical, rotating coordinate system in a form which is consistent with the shallow atmosphere approximation. (This point is discussed further by Veronis [21] and Phillips [22].) The equations of Phillips are modified in this report to conform with the UTM Cartesian coordinate system.

Since viscous effects are negligible in comparison with turbulence effects, the fluid is presumed to be inviscid. The equations of motion govern the behavior of the momentum:

$$m^i_t + \left[m^\alpha u^i - \tau^{\alpha i} + (\varepsilon + p)\delta^{\alpha i}\right]_\alpha + fm^\alpha \epsilon^{\alpha i 3} + \rho\Phi_i = 0 \tag{5}$$

where f is the Coriolis parameter; $\delta^{\alpha i}$ is the Kroneker delta which has the properties that $\delta^{ii} = 1$, $\delta^{\alpha i} = 0$, for $\alpha \neq i$; and $\epsilon^{\alpha i 3}$ is the skew-symmetric tensor which has the properties that $\epsilon^{123} = 1$, $\epsilon^{213} = -1$, and $\epsilon^{\alpha i 3} = 0$ for all other combinations of indices.

The most complicated equation is that for the total energy:

$$\left[\rho e + 1/2(\mu^\beta u^\beta + 3\varepsilon)\right]_t + \left[m^\alpha e + u^\alpha p + 3/2u^\alpha \varepsilon - \tau^{\alpha\beta}u^\beta + \Gamma^\alpha + c_v\zeta^\alpha\right]_\alpha = LC + Q \tag{6}$$

where e is the sum of the specific kinetic, geopotential, and internal energies, Q is the rate at which heat is added per unit volume by radiation and chemical processes, and LC is the rate at which latent heat is added by condensation of water vapor.

The continuity equation for water vapor is complicated by possible phase changes (condensation/evaporation) and the precipitation process. The simplest expression is that of the pseudoadiabatic process:

$$C + (\rho q)_t + n^\alpha_\alpha = 0, \tag{7}$$

where C is the rate of condensation.

In this simple expression, no attempt is made to conserve the nonvapor phases, which is equivalent to presuming immediate precipitation of all condensed water.

The basic equations which have been enumerated contain numerous esoteric turbulence terms which have been included for the sake of completeness. In practical applications of these equations, many of these terms can be ignored as they are insignificant in comparison with other terms.

Coordinate Transformation

The geopotential surfaces are not necessarily the most useful for defining the vertical coordinate. Kasahara [23] has recently reviewed the general class of coordinate transformations commonly used in atmospheric dynamics. Since the subject of this report is the dynamics of material layers, it is essential that a coordinate system be chosen so as to be consistent with mass conservation. As previously noted, there are naturally occurring, quasi-horizontal, material surfaces within the atmosphere which may be used for defining a nonorthogonal coordinate system which is naturally consistent with mass conservation.

Let $H(t,x,y)$ and $h(t,x,y)$ define the height of two quasi-horizontal surfaces in the atmosphere such that $H \geq h$. Between these surfaces is an atmospheric layer of thickness $D(t,x,y) \equiv H(t,x,y) - h(t,x,y) \geq 0$. For fixed horizontal coordinates, a new vertical coordinate is defined:

$$\sigma \equiv [z - h(t,x,y)]/D(t,x,y) \tag{8}$$

where $h \leq z \leq H$. If the surfaces of constant sigma are used as the vertical coordinate, the coordinate system is no longer orthogonal. Consequently, our differential equations must be altered to accommodate the change of coordinate.

From simple geometrical considerations, the following rules can be derived (see [23]).

$$C_i = C_i|_\sigma + C_z D\sigma_i, \quad i = 1,2 \tag{9a}$$

or

$$DC_i = (DC)_i|_\sigma + (CD\sigma_i)_\sigma, \quad i = 1,2 \tag{9b}$$

where C_i is the horizontal derivative of the arbitrary variable C in the i-th direction along a geopotential surface, $C_i|_\sigma$ is the partial derivative along the sigma surface, and $D\sigma_i$ pertains to the slope of the sigma surface in the i-th direction relative to the geopotential surface.

$$D\sigma_i = -(h_i + \sigma D_i),\ i = 1,2 \tag{10}$$

Now, consider the divergence of any arbitrary dependent vector ($a^i | i = 1,2,3$). From equation (9b)

$$Da^\alpha_\alpha = \left[(Da^x)_x + (Da^y)_y\right]|_\sigma + a^s_\sigma \ , \tag{11}$$

where

$$a^s \equiv a^z + D(a^x\sigma_x + a^y\sigma_y) \ . \tag{12}$$

The variable a^s is equal to the component of the vector normal to the sigma surface divided by cosine psi, where

$$\psi \equiv \tan^{-1}\left[D(a^x\sigma_x + a^y\sigma_y)\right]/(a^x a^x + a^y a^y)^{\frac{1}{2}} \ . \tag{13}$$

The change of vertical coordinate also necessitates a change in the definition of vertical motion. Formally

$$D\dot{\sigma} = w - (\dot{h} + \sigma\dot{D}) \ , \tag{14}$$

where the superior dot denotes the individual (or substantial) time derivative. The corresponding equation for the locally averaged "vertical" momentum is

$$\omega \equiv D\overline{\rho\dot{\sigma}} = m^z - \rho(\dot{h} + \sigma\dot{D}) = m^s - \rho(h_t + \sigma D_t) \ . \tag{15}$$

This last equation is the key expression of this report. If the sigma surface is a true material surface, that is, a surface through which there is no mass flux, then $\omega(\sigma) = 0$. Actually, there is no assurance that omega vanishes for all sigma values, but $\omega(1) = 0$ and $\omega(0) = 0$ if the layer is bounded by true material surfaces. For surfaces which are material surfaces in regard to transport, but not turbulent diffusion, one has $\dot{\sigma} = 0$ and $\omega = \mu^s$. Table 1 enumerates the basic equations following the transformations to the sigma coordinate system.

Material Layer Integral Operator

Let C denote any arbitrary dependent variable or expression. The simple material layer operator is defined to be the vertical integral, for fixed (x,y), of the integrand C over the thickness of the material layer between h and H; that is,

$$\langle C\rangle \equiv \int_{h(t,x,y)}^{H(t,x,y)} C(t,x,y,z)dz = D(t,x,y)\int_0^1 C(t,x,y,\sigma)d\sigma \tag{16}$$

TABLE 1. BASIC EQUATIONS IN MATERIAL LAYER COORDINATES

1. $$D\rho_t + [(Dm^x)_x + (Dm^y)_y]|_\sigma + m^s_\sigma = 0$$

2. $$Dm^x_t + \{[D(m^x u - \tau^{xx} + \varepsilon + p)]_x + [D(m^y u - \tau^{xy})]_y\}|_\sigma$$
$$- fDm^y + [m^s u - \tau^{xs} + (\varepsilon + p)D\sigma_x]_\sigma = 0$$

3. $$Dm^y_t + \{[D(m^x v - \tau^{xy})]_x + [D(m^y v - \tau^{yy} + \varepsilon + p)]_y\}|_\sigma$$
$$+ fDm^x + [m^s v - \tau^{ys} + (\varepsilon + p)D\sigma_y]_\sigma = 0$$

4. $$Dm^z_t + \{[D(m^x w - \tau^{xz})]_x + [D(m^y w - \tau^{yz})]_y\}|_\sigma$$
$$+ \rho\Phi_\sigma + [m^s w - \tau^{zs} + \varepsilon + p]_\sigma = 0$$

5. $$D[\rho e + 1/2(\mu^\beta u^\beta + 3\varepsilon)]_t + \{D[m^x e + up + 3/2u\varepsilon - \tau^{x\beta}u^\beta + \Gamma^x + c_v\zeta^x]\}_x|_\sigma$$
$$+ \{D[m^y e + vp + 3/2v\varepsilon - \tau^{y\beta}u^\beta + \Gamma^y + c_v\zeta^y]\}_y|_\sigma$$
$$+ \{m^s e + u^s p + 3/2u^s\varepsilon - \tau^{s\beta}u^\beta + \Gamma^s + c_v\zeta^s\}_\sigma$$
$$= D(Q + LC)$$

6. $$DC + D(\rho q)_t + [(Dn^x)_x + (Dn^y)_y]|_\sigma + n^s_\sigma = 0$$

Furthermore, the more general material layer moment operator is defined to be

$$\langle C|\eta\rangle \equiv D\int_0^1 C\sigma^{\eta}d\sigma \tag{17}$$

where η is a number greater than zero.

It is worthwhile to consider certain special cases. Making use of Leibnitz's rule, note that

$$\langle C_t\rangle = \langle C\rangle_t - C(t,x,y,H)H_t + C(t,x,y,h)h_t \ . \tag{18}$$

A similar expression applies to the moment operator. Because the derivatives are along the sigma surfaces, it is obvious that

$$\langle (DC)_i|_\sigma\rangle = D\langle C\rangle_i, \ i = 1,2 \tag{19}$$

A similar expression applies to the moment operator. Finally,

$$\langle C_\sigma\rangle = D[\,C(t,x,y,H) - C(t,x,y,h)\,] \tag{20a}$$

$$\langle C_\sigma|\eta\rangle = DC(t,x,y,H) - \eta\langle C|\eta-1\rangle \tag{20b}$$

The application of the integral operators to the equations of table 1 result in the material layer equations.

Material Layer Equations

Table 2 enumerates the complete elementary material layer equations. The normal momentum (ω) at the two bounding surfaces is included in the equations for completeness. However, these terms vanish when the bounding surfaces are material interfaces, which results in a significant simplification of the equations.

Because of equation (20b), moment equations always couple with the next lower-order moments. Table 3 presents examples of this coupling as manifested by the first-order moment material layer equations. Although the momentum normal to the sigma surfaces may vanish at the bounding surfaces for true material layers, there is no a priori assurance that this variable vanishes throughout the interior of the layer. Consequently, terms such as $\langle\omega\rangle$, $\langle\omega u\rangle$, $\langle\omega v\rangle$, etc., significantly complicate the moment material layer equations.

SOME PRACTICAL CONSIDERATIONS

If the formal theory of material layers were the only goal, tables 2 and 3 would suffice. However, any attempt to apply these equations would require additional relationships and/or approximations to effect closure.

TABLE 2. ELEMENTARY MATERIAL LAYER EQUATIONS

1. $\langle\rho\rangle_t + \langle m^x\rangle_x + \langle m^y\rangle_y + \omega(1) - \omega(0) = 0$

2. $\langle m^x\rangle_t + \langle m^x u - \tau^{xx} + \varepsilon + p\rangle_x + \langle m^y u - \tau^{yx}\rangle_y - f\langle m^y\rangle$

$$+ [\omega u - \tau^{sx} + (\varepsilon + p)D\sigma_x - \mu^x(h_t + \sigma D_t)]_0^1 = 0$$

3. $\langle m^y\rangle_t + \langle m^x v - \tau^{xy}\rangle_x + \langle m^y v - \tau^{yy} + \varepsilon + p\rangle_y + f\langle m^x\rangle$

$$+ [\omega v - \tau^{sy} + (\varepsilon + p)D\sigma_y - \mu^y(h_t + \sigma D_t)]_0^1 = 0$$

4. $\langle m^z\rangle_t + \langle m^x w - \tau^{xz}\rangle_x + \langle m^y w - \tau^{yz}\rangle_y + \langle\rho\rangle g$

$$+ [\omega w - \tau^{sz} + \varepsilon + p - \mu^z(h_t + \sigma D_t)]_0^1 = 0$$

5. $\langle \rho e + 1/2(\mu^\beta u^\beta + 3\varepsilon)\rangle_t + \langle m^x e + up + 3/2u\varepsilon - \tau^{x\beta}u^\beta + \Gamma^x + c_v\zeta^x\rangle_x$

$$+ \langle m^y e + vp + 3/2v\varepsilon - \tau^{y\beta}u^\beta + \Gamma^y + c_v\zeta^y\rangle_y$$

$$+ [\omega e + u^s p + 3/2u^s\varepsilon - \tau^{s\beta}u^\beta + \Gamma^s + c_v\zeta^s$$

$$- (\mu^\beta u^\beta + 3\varepsilon)\cdot(h_t + \sigma D_t)]_0^1 = \langle Q + LC\rangle$$

6. $\langle\rho q\rangle_t + \langle n^x\rangle_x + \langle n^y\rangle_y + [\omega q + \nu^s]_0^1 = -\langle C\rangle$

TABLE 3. FIRST-MOMENT MATERIAL LAYER EQUATIONS

1. $$\langle \rho|1\rangle_t + \langle m^x|1\rangle_x + \langle m^y|1\rangle_y + \omega(1) = \langle \omega\rangle/D$$

2. $$\langle m^x|1\rangle_t + \langle m^x u - \tau^{xx} + \varepsilon + p|1\rangle_x + \langle m^y u - \tau^{yx}|1\rangle_y - f\langle m^y|1\rangle$$
$$+ [\omega u - \tau^{sx} + (\varepsilon + p)H_x - \mu^x H_t]^{\sigma=1}$$
$$= \langle \omega u - \tau^{sx} - \mu^x(h_t + \sigma D_t) - (\varepsilon + p)\cdot(h_x + \sigma D_x)\rangle/D$$

3. $$\langle m^y|1\rangle_t + \langle m^x v - \tau^{xy}|1\rangle_x + \langle m^y v - \tau^{yy} + \varepsilon + p|1\rangle_y + f\langle m^x|1\rangle$$
$$+ [\omega v - \tau^{sy} + (\varepsilon + p)H_y - \mu^y H_t]^{\sigma=1}$$
$$= \langle \omega v - \tau^{sy} - \mu^y(h_t + \sigma D_t) - (\varepsilon + p)\cdot(h_y + \sigma D_y)\rangle/D$$

4. $$\langle m^z|1\rangle_t + \langle m^x w - \tau^{xz}|1\rangle_x + \langle m^y w - \tau^{yz}|1\rangle_y + \langle \rho|1\rangle g$$
$$+ [\omega w - \tau^{sz} + \varepsilon + p - \mu^z H_t]^{\sigma=1}$$
$$= \langle \omega w - \tau^{sz} - \mu^z(h_t + \sigma D_t) + \varepsilon + p\rangle/D$$

5. $$\langle \rho e + 1/2(\mu^\beta u^\beta + 3\varepsilon)|1\rangle_t + \langle m^x e + up + 3/2u\varepsilon - \tau^{x\beta}u^\beta + \Gamma^x + c_v\zeta^x|1\rangle_x$$
$$+ \langle m^y e + vp + 3/2v\varepsilon - \tau^{y\beta}u^\beta + \Gamma^y + c_v\zeta^y|1\rangle_y$$
$$+ [\omega e + u^s p + 3/2u^s\varepsilon - \tau^{s\beta}u^\beta + \Gamma^s$$
$$+ c_v\zeta^s - 1/2(\mu^\beta u^\beta + 3\varepsilon)\cdot(h_t + \sigma D_t)]^{\sigma=1}$$
$$= \langle Q + LC|1\rangle + \langle \omega e + u^s p + 3/2u^s\varepsilon$$
$$- \tau^{s\beta}u^\beta + \Gamma^s + c_v\zeta^s\rangle/D$$

6. $$\langle \rho q|1\rangle_t + \langle n^x|1\rangle_x + \langle n^y|1\rangle_y + [\omega q + \nu^s]^{\sigma=1} = \langle \omega q + \nu^s\rangle/D - \langle C|1\rangle$$

Closure is an imprecise process which develops by degrees depending on the nature of the problem addressed. There are any number of specialized applications for which the material layer equations are appropriate, but each involves a somewhat different closure process. This section considers some of the practical closure steps that would be common to many applications.

Turbulence Parameterization

In the context where they occur, a number of the turbulence terms are negligible. The turbulence pressure is insignificant in comparison with the pressure from the molecular motion. The horizontal turbulent mass flux (μ^x, μ^y) and heat flux (ζ^x, ζ^y) are negligible in comparison with the corresponding advective fluxes. Similar arguments can be used to eliminate other turbulence terms; however, the Reynolds stress and vertical turbulent heat and moisture flux terms may be significant factors, especially for a shallow material layer in juxtaposition with the earth's surface.

The turbulent heat flux (ζ^s) at the earth's surface is the principal source of diabatic effects on the atmosphere. The turbulent moisture flux (ν^s) is likewise the principal source of atmospheric water, and the Reynolds stress terms (τ^{xs}, τ^{ys}) at the earth's surface are the principal source of frictional effects on the atmosphere. The parameterization of these surface boundary variables is a closure problem common to many atmospheric models. Mellor and Yamada [24] have reported on a hierarchy of turbulence closure models for planetary boundary layers, and Yamada and Mellor [25] have discussed the validation of one of these models. Bhumralker [26] has recently reviewed several different schemes for boundary layer parameterization in atmospheric general circulation models, and Arya [27] has further discussed some of these approaches. Analogous closure schemes can be developed for the material layer equations, but the specific details are beyond the scope of this report.

There are several general considerations concerning turbulence effects on material layers. Material layers which are above the boundary layer usually have negligible turbulence effects (free atmosphere). Furthermore, it may be assumed that turbulence terms are negligible at the upper interface of a material layer even though it contains the boundary layer; in some cases, this may be true even if the upper interface is not a true material surface (entrainment). Note that as a consequence of this assumption the principal turbulent dissipation term ($\tau^{s\beta} u^{\beta}$) is ineffectual in the total energy equation (equation 5 of table 2) because $\tau^{s\beta}$ is assumed to vanish at the upper interface and, of course, u^{β} vanishes at the earth's surface because of the no-slip condition.

Although one may argue that the horizontal Reynolds stress terms are negligible in comparison with the advective momentum flux, there are pragmatic precedents which suggest that useful approximations of these turbulence effects can be made by the introduction of pseudoviscosity terms in the momentum equations. Consistent with this assumption would be the incorporation of a pseudoviscosity term into the energy equation to account for diffusion of kinetic energy.

The Hydrostatic Approximation

For many practical applications of the material layer equations, it is natural to resort to the usual hydrostatic approximation to aid the closure process. However, having eliminated the dynamic equation governing the vertical momentum, additional approximations must be introduced to allow evaluation of this important term. The most forthright approach to this problem is to presume that all sigma surfaces are material surfaces, that is, that the momentum normal to the sigma surfaces (ω) is everywhere negligible. There are situations, especially in complex terrain, where the conventional hydrostatic approximation and the latter premise are incongruous, but there is no straightforward substitute for the hydrostatic approximation which rectifies this problem.

The assumption of negligible momentum normal to the sigma surfaces within a material layer is a key consideration in the closure process of the material layer equations, especially in regard to the moment equations. Table 4 enumerates the elementary material layer equations which have been simplified by the general closure approximations considered to this point. Likewise, table 5 contains the simplified first-moment equations.

In these tables, $E \equiv \rho e$ and $K \equiv 1/2\rho u^{\beta}u^{\beta}$.

Prescribed Profiles

The material layer equations are nonlinear, that is, they contain higher-order terms involving products of variables. Consequently, some estimate of the vertical profile structure of the variables must be available to evaluate nonlinear terms. The matter of vertical profiles is not just a pedantic concern for detail. Profile interactions associated with nonlinear terms affect overall behavior of the material layers. In particular, the density (temperature) profile affects the buoyant stability of the material layer which, in turn, affects the kinematic variables. Unlike the shallow-fluid equations, the material layer equations recognize the compressibility of the atmosphere and the importance of thermodynamic effects. To capitalize on the improved generality of the material layer equations, one must be concerned about vertical profile structure, even if only rudimentarily.

Assume that the vertical profile of any state or kinematic variable within a material layer is smooth and can be approximated by a Taylor

TABLE 4. SIMPLIFIED ELEMENTARY MATERIAL LAYER EQUATIONS

1. $\langle\rho\rangle_t + \langle m^x\rangle_x + \langle m^y\rangle_y = 0$

2. $\langle m^x\rangle_t + \langle m^x u\rangle_x + \langle m^y u\rangle_y + \langle p\rangle_x - p(1)H_x$

$$+ p(0)h_x - f\langle m^y\rangle + \tau^{xs}(0) = k\nabla^2\langle m^x\rangle$$

3. $\langle m^y\rangle_t + \langle m^x v\rangle_x + \langle m^y v\rangle_y + \langle p\rangle_y - p(1)H_y$

$$+ p(0)h_y + f\langle m^x\rangle + \tau^{ys}(0) = k\nabla^2\langle m^y\rangle$$

4. $\langle\rho\rangle g + p(1) - p(0) = 0$

5. $\langle E\rangle_t + p(1)H_t - p(0)h_t + \langle u(E + p)\rangle_x$

$$+ \langle v(E + p)\rangle_y - c_p\zeta^s(0) = k\nabla^2\langle K\rangle + \langle Q + LC\rangle$$

6. $\langle\rho q\rangle_t + \langle n^x\rangle_x + \langle n^y\rangle_y - \nu^s(0) = -\langle C\rangle$

TABLE 5. SIMPLIFIED FIRST-MOMENT MATERIAL LAYER EQUATIONS

1. $\langle\rho|1\rangle_t + \langle m^x|1\rangle_x + \langle m^y|1\rangle_y = 0$

2. $\langle m^x|1\rangle_t + \langle m^x u|1\rangle_x + \langle m^y u|1\rangle_y + \langle p|1\rangle_x - p(1)H_x - f\langle m^y|1\rangle$

$$= k\nabla^2\langle m^x|1\rangle - (\langle p\rangle h_x + \langle p|1\rangle D_x)/D$$

3. $\langle m^y|1\rangle_t + \langle m^x v|1\rangle_x + \langle m^y v|1\rangle_y + \langle p|1\rangle_y - p(1)H_y + f\langle m^x|1\rangle$

$$= k\nabla^2\langle m^y|1\rangle - (\langle p\rangle h_y + \langle p|1\rangle D_y)/D$$

4. $\langle\rho|1\rangle g + p(1) = \langle p\rangle/D$

5. $\langle E|1\rangle_t + p(1)H_t + \langle u(E + p)|1\rangle_x + \langle v(E + p)|1\rangle_y$

$$= k\nabla^2\langle K|1\rangle + \langle Q + LC|1\rangle + [c_p\langle\zeta^s\rangle$$

$$+ \langle p\rangle h_t + \langle p|1\rangle D_t - \langle\tau^{s\beta}u^\beta\rangle]/D$$

6. $\langle\rho q|1\rangle_t + \langle n^x|1\rangle_x + \langle n^y|1\rangle_y = -\langle C|1\rangle + \langle\nu^s\rangle/D$

series with "negligible" remainder. Consequently, the profile can be represented by a polynomial of some finite degree, say n. This approach parallels that used for the development of multilevel numerical atmospheric models where such Taylor expansions are used to derive finite-difference analogs of the partial derivatives of the model equations. The end result of such numerical models is the expression of the vertical distribution in terms of discrete values at each level in the numerical model. The continuous profile may be constructed from these discrete values by Newton or Lagrange interpolation. On the other hand, if one applies the material layer operator for n + 1 moments to the n-degree polynomial, a system of linear equations is derived which relate the profile coefficients to the moments. Thus, on the one hand the model resolution is determined by the number of levels and on the other by the number of moments evaluated.

Profile description does not have to be restricted to polynomials; any integrable function can be used. For example, since a power-law is commonly used to approximate the wind profile in the boundary layer, this would be a more logical choice than a zero- or first-order polynomial. On the other hand, the combination of the hydrostatic approximation and the equation of state restricts the degrees of freedom for characterizing the profiles of state variables. The simplest, nontrivial case is a polytropic representation.

To this point, only profiles within a material layer have been discussed. If the atmosphere is composed of several overlapping material layers, the complete profile is pieced together from the profiles of each layer. At the interface between material layers, the dynamic boundary condition must be satisfied. (The kinematic boundary condition is met a priori.) Indeed, it is natural to require continuity of all variables across the interface. However, there are practical reasons for relaxing the requirement of continuity.

Consider a hypothetical case where the atmospheric structure in a given region consists of a single subsidence inversion imbedded in an otherwise comparatively labile troposphere. Most likely, the vertical distribution of moisture and pollution would reveal that there is a material layer below the subsidence inversion. Likewise, the layer between the subsidence inversion and the tropopause would be another material layer. Profiles within these layers could be approximated by low-order polynomials provided no portion of the subsidence inversion is incorporated into the layers. To complete the continuous profile, it is necessary to include the subsidence inversion layer as a third material layer buffer between the upper and lower layers.

Numerous situations arise as described above, where comparatively thick material layers are separated by a stable layer which is thin but still significant in terms of profile structure. Because of the almost insig-

nificant thickness of these layers, it is desirable to approximate these layers by an infinitesimally thin interfacial layer. In considering the dynamic boundary condition in relation to the equations of table 4, the following diagnostic equation has been derived to govern the interfacial values.

$$\left[1/2(\overline{m^x u}\Delta u + \overline{m^x v}\Delta v) + (c_p/R)p\Delta u + c_p\overline{m^x}\Delta T\right]_x + \left[1/2(\overline{m^y u}\Delta u + \overline{m^y v}\Delta v)\right.$$

$$\left. + (c_p/R)p\Delta v + c_p\overline{m^y}\Delta T\right]_y = 0 \qquad (21)$$

In this equation, ΔT, Δu, and Δv are the magnitude of the jump discontinuities of temperature and velocity across the interface and the superior bar denotes "average" values of the variables within the infinitesimal interfacial layer. For practical purposes, these quantities are the average of the appropriate upper and lower interfacial values.

The introduction of interfacial discontinuities is an artifice but is of practical value in simplifying the modeling of material layer behavior. Equation (21), which is a generalized representation of Margules' equation, allows for a physically meaningful control over the magnitude of the jumps.

The piecewise construction of vertical profiles generally requires a knowledge of the variables, or quantitative relationships which govern their behavior, at the upper and lower bounding interfaces as well as the internal interfaces.

Bounding Passive Layer

For most practical applications, it is neither necessary nor desirable to apply the material layer equations to the entire depth of atmospheric mass. Most problems of interest are confined to the troposphere. Under these circumstances, it is necessary to introduce a superior bounding layer which is more or less passive in relation to the material layer effects which occur below. Since the objective is to establish the requisite boundary conditions at the uppermost material interface, the prescription of the structure of the passive layer need not be in any greater detail than that required to achieve the objective.

For the first example of a passive bounding layer, consider a hypothetical stratosphere which is isothermal. According to the hydrostatic equation, the pressure and density profiles have exponential decay with height and there is no distinct "top" for the atmosphere. Since no thermal wind exists in this hypothetical stratosphere, it is reasonable to assume that the wind is constant with height. It is readily shown that knowledge of the state and kinematic variables on the tropopause is sufficient to allow specification of all variables throughout the stratosphere.

Table 6 enumerates a system of equations governing the state and kinematic variables on the tropopause below an isothermal stratosphere with prescribed geostrophic wind (u_g, v_g). Here, H and p are the height and pressure, respectively, of the tropopause and all space derivatives pertain to the tropopause surface. The solution of these equations provides the requisite interfacial values to couple with the tropospheric profiles.

Further simplifications of the passive isothermal layer may be effected by assuming the stratospheric wind (including the tropopause) to be geostrophic. In either case, the isothermal assumption may be crude but not unreasonable, and should serve well for establishing tropopause values for a tropospheric material layer model. A more general model is achieved by using the isothermal stratospheric model to specify upper interfacial values in conjunction with the incorporation of equation (21) into the model.

The simplest possible example of a passive bounding layer within the troposphere is one assumed to be adiabatic with the wind uniformly geostrophic. The bounding interface is presumed to be an isentropic surface and consequently the Montgomery streamfunction ($gH + c_pT$) is a linear function of position on the interface (as a consequence of the geostrophic wind assumption). The wind and temperature profiles within the inferior material layer must be defined so as to approach, as $\sigma \to 1$, the geostrophic wind and the temperature consistent with the Montgomery streamfunction relationship alluded to above. Again, a more general model is achieved by using the adiabatic layer model to prescribe the upper interfacial values for use in equation (21).

The examples of upper boundary conditions described above are only two of many possible alternatives; the choice depends upon the application to be made of the material layer equations. A major point to note is how additional degrees of freedom are allowed for the material layer solutions by use of the generalized Margules equation (21), which is a diagnostic equation and thus readily used in numerical models.

Air/Earth Interface

Air/earth interaction at the ground surface is intimately related to the problem of boundary layer turbulence; however, it is beyond the scope of this report to present detailed air/earth interaction relationships for application to material layer models. Regardless of the detailed approach used, the kinematic variables must vanish at the air/earth interface in accordance with the no-slip condition, and the temperature (and specific humidity) must be prescribed or evaluated from an appropriate surface energy budget model.

The boundary conditions at the air/earth interface are a problem common to many atmospheric prediction models. For example, Bhumralker [28] has

TABLE 6. TROPOPAUSE EQUATIONS FOR ISOTHERMAL STRATOSPHERE

$$p_t + up_x + vp_y = 0$$

$$p_x/\rho + gH_x - fv_g = 0$$

$$p_y/\rho + gH_y + fu_g = 0$$

$$u_t + uu_x + vu_y - f(v - v_g) = 0$$

$$v_t + uv_x + vv_y + f(u - u_g) = 0$$

$$u_x + v_y = 0$$

described a hierarchy of numerical algorithms for the computation of ground surface temperature in an atmospheric general circulation model, and Deardorff [29] has further developed this approach to include a layer of vegetation. In arriving at an appropriate air/earth interaction model, a critical decision must be made as to whether the evaluation of the soil heat flux requires that the "soil temperature" be prescribed. A prescribed soil temperature provides negative feedback to an energy budget model which assures reasonably predicted surface conditions (provided the specified soil temperature is reasonable).

The Bhumralker/Deardorff approach can be generalized for use with material layer equation models, but for complex terrain the specification of the many esoteric parameters, least of all "soil temperature," may be by guess. Under these circumstances, it might be just as well to prescribe outright the interface temperature and thus forego the complexities of a surface energy budget model of questionable validity.

MATERIAL LAYER MODELS

The central theme of this report is the theoretical development of the material layer equations and the associated problems of closure. Examples of material layer models are presented in this section to demonstrate various specialized applications of the material layer equations. Although numerical algorithms are not presented in support of the examples, the utility of the sample material layer models should be evident.

The first example is presented as the material layer analog of the conventional one-layer shallow-fluid equation terrain effects model. The second example is an extremely simple model to demonstrate the utility of the material layer equations when the bounding interface is not a material surface. Finally, the third example deals with the use of the material layer equations for diagnostic analysis of terrain effects on atmospheric phenomena using a variational approach.

An Elementary Mixing Layer Model

Tingle and Bjorklund [5] have described a mixing layer model based upon the shallow-fluid equations; the objective here is to present the basis for a mixing layer model derived from the material layer equations. Although intended as the compressible fluid analog of the shallow-fluid equations, a comparison of the two approaches is like that of apples to oranges. However, it is appropriate to consider this as the basis for further generalization of the Tingle-Bjorklund model to incorporate, among other things, thermodynamic effects on mixing layer dynamics.

The mixing layer is defined to be the primary material layer in juxtaposition with the ground. It may be a rather deep labile layer capped by an elevated subsidence inversion or a shallow stable layer confined to a nocturnal surface inversion. Since only a one-layer model is being

considered, the isentropic, geostrophic material interface described in "Bounding Passive Layer" is chosen as the upper boundary condition. The layer structure is assumed to be polytropic (linear temperature profile). The "ground" temperature could be implicitly evaluated if there was provision for an air/earth interaction model. However, for this elementary mixing layer model, it shall be assumed that the "ground" temperature is steady and everywhere prescribed and that the turbulent heat flux at the ground $[\zeta^s(0)]$ is negligible. Table 7 enumerates the relationships governing the layer structure. Table 8 lists the boundary conditions at the air/earth interface, and table 9 itemizes the boundary conditions at th upper isentropic, geostrophic surface. Finally, table 10 enumerates the material layer equations for the elementary mixing layer model.

Aside from the coriolis force, surface drag, and pseudoviscosity terms which the Tingle-Bjorklund model neglects, the first three equations of table 10 are analogous to those of Tingle-Bjorklund provided that the density is assumed constant and the vertical profile of velocity is uniform. The term $gD(\langle\rho|1\rangle - 1/2\hat{\rho}D)$ is analogous to the Tingle-Bjorklund term $1/2g'D^2$, which is the square of the gravity wave speed, where $g' \sim g(\rho - \hat{\rho})/\rho$ is the reduced gravity. The Tingle-Bjorklund model has no counterpart to equation 4 of table 10.

Several points should be made concerning the derivation of equation 4 of table 10. First, there are no time derivatives of the temperature because of the manner in which the upper and lower boundary conditions were stated. Furthermore, the first moment of the continuity equation was used in deriving equation 4. However, the main point is that, by comparison with the shallow-fluid equations, the fourth equation introduces a whole new perspective to terrain and thermodynamic effects on mixing layer dynamics.

The use of the isentropic, geostrophic upper material interface would be most appropriate for the case of a mixing layer associated with a surface-based inversion. On the other hand, if the upper material interface is the base of an elevated inversion, a more general model is achieved by the use of equation (21) wherein the isentropic, geostrophic assumption pertains only to the upper interface. Furthermore, equation (21) would be modified for the simplest model by assuming uniformity in the interfacial layer, that is

$$1/2(\overline{m^x u}\Delta u + \overline{m^x v}\Delta v) + (c_p/R)p\Delta u + c_p\overline{m^x}\Delta T = \text{constant} \qquad (22a)$$

$$1/2(\overline{m^y u}\Delta u + \overline{m^y v}\Delta v) + (c_p/R)p\Delta v + c_p\overline{m^y}\Delta T = \text{constant} \qquad (22b)$$

The profile relationships of table 7 must be modified to reflect values at the upper boundary of the mixing layer consistent with the lower interfacial values derived from equations (22a) and (22b). Although

TABLE 7. LAYER STRUCTURE FOR ELEMENTARY MIXING-LAYER MODEL

1. Lapse Rate

$$\gamma = -T_z = [T(0) - T(1)]/D$$

2. Polytropic Pressure Profile

$$p(\sigma) = p(0)[T(\sigma)/T(0)]^{\delta}, \text{ where } \delta = g/R\gamma$$

3. Linear Temperature Profile

$$T(\sigma) = T(0) - \gamma D\sigma$$

4. Pressure Integral

$$\langle p \rangle = D[g\langle \rho | 1 \rangle + p(1)] = R[(\langle \rho \rangle - \langle \rho | 1 \rangle)T(0) + \langle \rho | 1 \rangle T(1)]$$

5. Prescribed Power-Law Mixing-Layer Wind Profile

$$u(\sigma) = u_o \sigma^{\eta}(1-\sigma) + \hat{u}\sigma$$

$$v(\sigma) = v_o \sigma^{\eta}(1-\sigma) + \hat{v}\sigma$$

where η is prescribed.

TABLE 8. BOUNDARY CONDITIONS AT THE AIR/EARTH INTERFACE

1. Temperature Prescribed

$$T(0) = \tilde{T}(x,y)$$

2. No-Slip Condition

$$u(0) = v(0) = 0$$

3. Form Drag Relationship For Surface Reynolds Stress

$$\tau^{xs}(0) = du_o \ , \ \tau^{ys}(0) = dv_o \ ,$$

where d is also a function of u_o, v_o and the surface roughness.

4. Negligible Heat Exchange

$$\zeta^s(0) \simeq 0$$

TABLE 9. BOUNDARY CONDITIONS AT UPPER ISENTROPIC GEOSTROPHIC SURFACE

1. Montgomery Streamfunction Relationship

$$gH + c_p T(1) = (g\hat{H} + c_p \hat{T}) + f(\hat{v}x - \hat{u}y) ,$$

where $(g\hat{H} + c_p \hat{T})$ is a nominal (constant) Montgomery streamfunction, and $\hat{u}$, $\hat{v}$ are the (constant) geostrophic wind components.

2. Pressure Relationship

$$p_o \Pi(1) = p_o [p(1)/p_o]^{R/c_p} = RrT(1)$$

where r is the potential density of the isentropic surface.

3. Wind Relationship

$$u(1) = \hat{u} , \quad v(1) = \hat{v}$$

TABLE 10. MATERIAL LAYER EQUATIONS FOR ELEMENTARY MIXING-LAYER MODEL

1. $\langle\rho\rangle_t + \langle m^x\rangle_x + \langle m^y\rangle_y = 0$

2. $\langle m^x\rangle_t + \langle m^x u\rangle_x + \langle m^y u\rangle_y + g[D(\langle\rho|1\rangle - 1/2\hat{\beta}D)]_x$

$$+ g[\langle\rho\rangle - \hat{\beta}D]h_x - f(\langle m^y\rangle - \hat{\beta}D\hat{v}) + du_o = k\nabla^2\langle m^x\rangle$$

3. $\langle m^y\rangle_t + \langle m^x v\rangle_x + \langle m^y v\rangle_y + g[D(\langle\rho|1\rangle - 1/2\hat{\beta}D)]_y$

$$+ g[\langle\rho\rangle - \hat{\beta}D]h_y + f(\langle m^x\rangle - \hat{\beta}D\hat{u}) + dv_o = k\nabla^2\langle m^y\rangle$$

4. $[\langle K\rangle - gD(\langle\rho|1\rangle - 1/2\hat{\beta}D)]_t + \langle uK\rangle_x + \langle vK\rangle_y$

$$+ (\langle m^x\rangle - \langle m^x|1\rangle)\cdot(gh + c_p\tilde{T})_x$$

$$+ (\langle m^y\rangle - \langle m^y|1\rangle)\cdot(gh + c_p\tilde{T})_y$$

$$+ f[\langle m^x|1\rangle\hat{v} - \langle m^y|1\rangle\hat{u}] = k\nabla^2\langle K\rangle$$

this further complicates the solution of the model equations, additional degrees of freedom are provided for profile evaluations without the introduction of additional dynamic differential equations.

Mixing Layer Entrainment Model

The presence of an inversion does not necessarily assure the existence of a material layer. The processes of penetrative convection and entrainment invalidate the premise of mass conservation. In the case of penetrative convection, organized convective elements have sufficient buoyancy to "punch holes" in the inversion. The inversion is more like a sieve than a lid, and consequently it is difficult to reconcile the material layer equations with the condition of penetrative convection. In the case of entrainment, one or both layers adjacent to the inversion are turbulent with the result that the turbulence erodes away the inversion layer with an associated entrainment of mass at the expense of the inversion layer.

The classical example of entrainment is the burning-off of a nocturnal surface inversion after sunrise. The solar heating leads to a mixing layer which deepens with time and eventually wipes out the inversion layer. To illustrate this, consider a simple case with calm wind and horizontal homogeneity. The behavior of the mixing layer is described by the following equations:

$$\langle \rho \rangle_t + \omega(1) = 0 \tag{23}$$

$$\langle p \rangle_t + R[\omega(1)T(1) + \zeta^s(1)] = R\zeta^s(0) \tag{24}$$

where $-\omega(1)$ is the rate of mass entrainment, $\zeta^s(1)$ and $\zeta^s(0)$ pertain to the turbulent heat flux at the bottom and the top of the mixing layer, respectively. If the layer above the inversion is a nonturbulent material layer, the combined mixing layer and inversion layer is also a material layer (this is the difference between entrainment and penetrative convection). The material layer equations for the combined mixing/inversion layer are

$$\langle \rho \rangle_t = 0 \tag{25}$$

$$\langle p \rangle_t = R\zeta^s(0) \tag{26}$$

This formulation of the problem should be compared to that given by Tennekes [30]. To facilitate this comparison, it is assumed that the mixing layer has a dry adiabatic lapse rate. Consequently

$$\langle p \rangle_{\text{Mixing layer}} = (p(0)T(0) - p(1).T(1))/(g/R + g/c_p). \tag{27}$$

The interior of the inversion layer is assumed nonturbulent and adiabatic with respect to time (up to the time the inversion is annihilated). For the sake of simplicity, assume that the lapse rate within the inversion layer is a constant. Because of the hydrostatic and adiabatic assumptions, the lapse rate within the inversion layer is constant in time as well as space. It follows from the preceding that

$$\zeta^s(1) = 0 \tag{28}$$

and

$$\omega(1) = p(1)\zeta^s(0)/(\gamma - g/c_p)\langle p\rangle_{\text{Mixing layer}} \tag{29a}$$

$$\simeq \zeta^s(0)/(\gamma - g/c_p)D \tag{29b}$$

where γ is the lapse rate in the inversion layer. Combining equations (23) and (29b), one may derive the approximate relationship

$$(D^2)_t \simeq -2\zeta^s(0)/\bar{\rho}(\gamma - g/c_p) \tag{30}$$

where $\bar{\rho}$ is the mean mixing layer density. For a steady surface heat flux, equation (30) is in consonance with the square-root-of-time relationship for the evaluation of the mixing layer depth (see equation (19) of Tennekes [30]).

The material layer approach to the problem of daytime mixing layer evolution is quite formal but straightforward. There are significant differences between this approach and that of Tennekes [30], but comparison is difficult. Tennekes speaks of entrainment and penetrative convection as if they were the same process, possibly because he introduces the artifice of characterizing the inversion layer as a jump discontinuity rather than a layer of finite thickness.

The elementary model of daytime mixing layer evolution given above is one example of the utility of the material layer equations even when the condition of mass continuity is negated. Similar "leaky" material layer applications are: the opposite problem of the evolution of the nocturnal surface inversion layer, the more general problem of nocturnal air drainage, and the related problem of diurnal slope winds associated with surface heating.

Variational Material Layer Model

Once suitable lateral boundary conditions are established, the mixing layer model set forth in "An Elementary Mixing Layer Model" becomes a

deterministic initial-value problem which is most suitable for prognostication. Even so, models of this type have also been used for diagnostic analysis [3,4,5]. However, there are definite problems in the use of wholly deterministic models for diagnostic analysis since any attempt to constrain the model solution to conform to observational input data (except for boundary and initial conditions) may lead to an ill-posed problem. In this case, variational analysis may be used to draw a compromise between model equations and observational input data for diagnostic analysis.

Ohmstede [31] and Meyers, Cedarwall, and Ohmstede [32] have reported on a model for diagnostic analysis of terrain effects on atmospheric phenomena using a variational approach. This model is so straightforward that its principles are readily summarized here. At any one time, the model deals with a single material layer of thickness $D(x,y) > 0$ in juxtaposition with the ground. The material layer variables subjected to variational adjustment are the depth of the layer, the zero- and first-order moments of the mass flux vector, the total energy flux vector, and the potential energy flux vector. The height of the ground is prescribed.

The general concepts of the variational analysis begin with some simply connected region for which analysis is desired. Using the limited observations available, some form of objective analysis is used to construct fields of the relevant variables within the region. These are called the "observed" fields even though the only observations are actually at discrete space/time points. Only in a very limited way do the observed fields reflect terrain effects. Consequently, the desire is to construct, by means of variational analysis, new fields which better characterize the terrain effects but still are in consonance with the observed fields in a least-squared sense. The object is to minimize the square-variation of the field variables but subject to functional constraints which manifest terrain effects. The constraints used are the dynamic equations 1 and 5 of table 4 and equation 1 of table 5, and two algebraic equations which characterize the interdependence of the variables. The resultant variational fields of this analysis model are the observed fields adjusted to comply with the material layer constraints.

Many different variational models are possible using the material layer equations. More advanced models should consider multilayer interactions and the use of the momentum equations.

CONCLUSIONS

The objective of this report has been to set forth new tools for atmospheric diagnostic/prognostic analysis. It could be argued that the material layer equations are not really new but just a further generalization of the shallow-fluid equations. Although largely true, the material layer equations contain unique features which are entirely overlooked by the incompressible shallow-fluid approach.

The material layer approach is most useful when the matter of concern is the transport and diffusion of material such as from NBC weapons or smoke. Equally important, however, are the features of the material layer approach which allow a more general analysis of the interaction of terrain and thermodynamic effects. Although the material layer equations could surely be used for prognosis if suitable initial and boundary conditions could be established, it is believed that their greatest utility is likely to be for mesoscale diagnostic analysis of terrain and thermodynamic effects using a variational approach.

REFERENCES

1. "Tactical Environmental Support System," 1976, USAICS, TRADOC.

2. Meyers, R. E., and R. E. Dettling, 1973, "A Simplified Orostrophic Adjustment Model," Technical Report, Dugway Proving Ground, Dugway, UT.

3. Tingle, A. G., and J. R. Bjorklund, 1973, "Simulation of Mesoscale Winds over Complex Terrain Using a Three-Layer Shallow-Fluid Analogy," Technical Report, Dugway Proving Ground, Dugway, UT.

4. Tingle, A., and J. Bjorklund, 1973, "Study and Investigation of Computer Algorithms for the Solution of the Shallow-Fluid Equations As a Means of Computing Terrain Influences on Wind Fields," Final Report, Contract No. DAAD07-72-C-0309, Atmospheric Sciences Laboratory, US Army Electronics Command, White Sands Missile Range, NM.

5. Dumbauld, R. K., and J. R. Bjorklund, 1977, "Mixing-Layer Analysis Routine and Transport/Diffusion Application Routine for EPAMS," Final Report, Contract No. DAAD07-76-C-0023, Atmospheric Sciences Laboratory, US Army Electronics Command, White Sands Missile Range, NM.

6. Freeman, J., 1973, "The ISR Diagnostic and Prediction Mesoscale Meteorological System," Final Report, Contract No. DAAD-05-72-C-0130.

7. Bjerknes, J., and H. Solberg, 1920, "Life Cycle of Cyclones and the Polar Front Theory," Geofy. Publ., 2(3).

8. Shuman, F., and J. Hovermale, 1968, "An Operational 6-Layer Primitive Equation Model," J. Appl. Meteorol., 7:525-547.

9. Freeman, J., 1952, "Flow Under an Inversion of Middle Latitudes," Ph.D. Dissertation, University of Chicago.

10. Tepper, M., 1952, "The Application of the Hydraulic Analogy to Certain Atmospheric Flow Problems," Department of Commerce, Weather Bureau Research Paper No. 35.

11. Houghton, D., and A. Kasahara, 1968, "Nonlinear Shallow-Fluid Flow Over an Isolated Ridge," Commun. Pure Appl. Math., 21:1-23.

12. Long, R., 1972, "Finite Amplitude Disturbances in the Flow of Inviscid Rotating and Stratified Fluids over Obstacles," Ann. Rev. Fluid. Mech., 4:69-92.

13. Stoker, J., 1957, Water Waves, Interscience Publishers, New York.

14. Stoker, J., 1953, "Dynamic Theory for Treating the Motion of Cold and Warm Fronts in the Atmosphere," Inst. Math. Sci., NYU, Report IMM-195.

15. Kasahara, A., E. Isaacson, and J. Stoker, 1965, "Numerical Studies of Frontal Motion in the Atmosphere," Tellus, 17:261-276.

16. Turkel, E., 1970, "Frontal Motion in the Atmosphere," Inst. Math. Sci., NYU, Report IMM-385.

17. Lavoie, R., 1972, "A Mesoscale Numerical Model of Lake-Effect Storms," J. Atmospheric Sci., 29:1025-1040.

18. Lax, P., and B. Wendorf, 1960, "Systems of Conservation Laws," Commun. Pure Appl. Math., 13:217-237.

19. Sundstrom, A., 1973, "Theoretical and Practical Problems in Formulating Boundary Conditions for a Limited-Area Model," Report DM-9, Institute of Meteorology, University of Stockholm.

20. Phillips, N., 1966, "The Equations of Motion for a Shallow Rotating Atmosphere and the 'Traditional Approximation'," J. Atmospheric Sci. 23:626-628.

21. Veronis, G., 1968, "Comments on Phillips Proposed Simplification of the Equations of Motion for a Shallow Rotating Atmosphere," J. Atmospheric Sci., 25:1154-1155.

22. Phillips, N., 1968, "Reply," J. Atmospheric Sci., 25:1155-1157.

23. Kasahara, A., 1974, "Various Vertical Coordinate Systems Used for Numerical Weather Prediction," Monthly Weather Rev., 102:509-522.

24. Mellor, G. L., and T. Yamada, 1974, "A Hierarchy of Turbulence Closure Models for Planetary Boundary Layers," J. Atmospheric Sci., 3:1791-1806.

25. Yamada, T., and G. Mellor, 1975, "A Simulation of the Wangara Atmospheric Boundary Layer Data," J. Atmospheric Sci., 32:2309-2329.

26. Bhumralker, C. M., 1976, "Parameterization of the Planetary Boundary Layer in Atmospheric General Circulation Models - A Review," Rev. Geophys. Space Phys., 14:215-226.

27. Arya, S. P. S., 1977, "Suggested Revisions to Certain Boundary Layer Parameterization Schemes Used in Atmospheric Circulation Models," Monthly Weather Rev., 105:215-227.

28. Bhumralker, C. M., 1975, "Numerical Experiments on the Computation of Ground Surface Temperature in an Atmospheric General Circulation Model," J. Appl. Meteorol., 14:1246-1258.

29. Deardorff, J. W., 1978, "Efficient Prediction of Ground Surface Temperature and Moisture, With Inclusion of a Layer of Vegetation," J. Geophys. Res., 83:1889-1904.

30. Tennekes, H., 1973, "A Model for the Dynamics of the Inversion Above a Convective Boundary Layer," J. Atmospheric Sci., 30:558-567.

31. Ohmstede, W. D, 1977, "Diagnostic Analysis of Terrain Effects on Atmospheric Phenomena Using a Variational Approach," Proceedings of the 7th Technical Exchange Conference, El Paso, TX, Atmospheric Sciences Laboratory, US Army Electronics Command, White Sands Missile Range, NM.

32. Meyers, R. E., R. T. Cedarwall, and W. D. Ohmstede, "Modeling Regional Atmospheric Transport and Diffusion: Some Environmental Application," Advances in Environmental Science and Engineering, Gordon and Breach, Science Publishers, Inc., NY. (in press)

GLOSSARY OF SYMBOLS

Symbol	Units	Meaning
C	kgm/m^3-sec	Rate of water condensation
C_D	-	Drag coefficient
c_p	j/kgm-deg	Specific heat at constant pressure
c_v	j/kgm-deg	Specific heat at constant volume
$d = 1/2\rho(0)C_D(u_o^2 + v_o^2)^{\frac{1}{2}}$	kgm/m^2-sec	Surface stress coefficient
D	m	Depth of material layer
$e = 1/2u^\beta u^\beta + \Phi + c_vT$	j/kgm	Specific total energy
$E = \rho e$	j/m^3	Volumetric total energy
f	rad/sec	Coriolis parameter
g	m/sec^2	Acceleration of gravity
h	m	Elevation of base of material layer
H	m	Elevation of top of material layer
k	m^2/sec	Pseudoviscosity
$K = 1/2\rho u^\beta u^\beta$	j/m^3	Kinetic energy
L	j/kgm	Heat of vaporization
m^i	kgm/m^2-sec	Momentum component in i-th direction
n^i	kgm/m^2-sec	Water vapor flux component in the i-th direction
P	Pascals	Pressure
P_o	Pascals	Reference pressure
q	kgm/kgm	Specific humidity
Q	$Watts/m^3$	Heating rate due to radiation and chemical processes
r	kgm/m^3	Potential density
R	j/kgm-deg	Gas constant
s	-	Superscript denoting coordinate direction normal to σ-surfaces
t	sec	Time
T	deg K	Temperature
$\tilde{T}$	deg K	Ground temperature

$\hat{u}^i$	m/sec	Turbulent velocity fluctuation in i-th direction
u	m/sec	Velocity component in X-direction
v	m/sec	Velocity component in Y-direction
w	m/sec	Velocity component in Z-direction
x^i	m	Coordinate in i-th direction
x	m	UTM grid easting
y	m	UTM grid northing
z	m	Elevation
α	-	Coordinate index requiring summation convention
β	-	Coordinate index requiring summation convention
γ	deg/m	Lapse rate
$\Gamma^i = 1/2\rho\overline{\hat{u}^i\hat{u}^\beta\hat{u}^\beta}$	j/m^2-sec	Turbulent transfer of turbulent kinetic energy
δ^{ij}	-	Kroneker delta
$\varepsilon = 1/3\rho\overline{\hat{u}^\beta\hat{u}^\beta}$	Pascals	Turbulence pressure
$\epsilon^{\alpha i 3}$	-	Skew-symmetric tension
$\zeta^i = \overline{\rho\hat{u}^i\hat{T}}$	kgm-deg/m^2-sec	Turbulent heat flux in i-th direction
$\mu^i = \overline{\rho\hat{u}^i}$	kgm/m^2-sec	Turbulent mass flux in i-th direction
$\nu^i = \overline{\rho q\hat{u}^i}$	kgm/m^2-sec	Turbulent water vapor flux in i-th direction
Π	-	Adiabatic reduced pressure
ρ	kgm/m^3	Density
σ	-	Material layer vertical coordinate
$\tau^{ij} = -\rho\hat{u}^i\hat{u}^j + \delta^{ij}\varepsilon$	Newton s/m^3	Reynolds' stress tensor
$\Phi = gz$	j/kgm	Geopotential
ω	kgm/m^2-sec	Momentum component normal to σ-surfaces

DISTRIBUTION LIST

Dr. Frank D. Eaton
Geophysical Institute
University of Alaska
Fairbanks, AK 99701

Commander
US Army Aviation Center
ATTN: ATZQ-D-MA
Fort Rucker, AL 36362

Chief, Atmospheric Sciences Div
Code ES-81
NASA
Marshall Space Flight Center,
AL 35812

Commander
US Army Missile R&D Command
ATTN: DRDMI-CGA (B. W. Fowler)
Redstone Arsenal, AL 35809

Redstone Scientific Information Center
ATTN: DRDMI-TBD
US Army Missile R&D Command
Redstone Arsenal, AL 35809

Commander
US Army Missile R&D Command
ATTN: DRDMI-TEM (R. Haraway)
Redstone Arsenal, AL 35809

Commander
US Army Missile R&D Command
ATTN: DRDMI-TRA (Dr. Essenwanger)
Redstone Arsenal, AL 35809

Commander
HQ, Fort Huachuca
ATTN: Tech Ref Div
Fort Huachuca, AZ 85613

Commander
US Army Intelligence Center & School
ATTN: ATSI-CD-MD
Fort Huachuca, AZ 85613

Commander
US Army Yuma Proving Ground
ATTN: Technical Library
Bldg 2100
Yuma, AZ 85364

Naval Weapons Center (Code 3173)
ATTN: Dr. A. Shlanta
China Lake, CA 93555

Sylvania Elec Sys Western Div
ATTN: Technical Reports Library
PO Box 205
Mountain View, CA 94040

Geophysics Officer
PMTC Code 3250
Pacific Missile Test Center
Point Mugu, CA 93042

Commander
Naval Ocean Systems Center (Code 4473)
ATTN: Technical Library
San Diego, CA 92152

Meteorologist in Charge
Kwajalein Missile Range
PO Box 67
APO San Francisco, CA 96555

Director
NOAA/ERL/APCL R31
RB3-Room 567
Boulder, CO 80302

Library-R-51-Tech Reports
NOAA/ERL
320 S. Broadway
Boulder, CO 80302

National Center for Atmos Research
NCAR Library
PO Box 3000
Boulder, CO 80307

R. B. Girardo
Bureau of Reclamation
E&R Center, Code 1220
Denver Federal Center, Bldg 67
Denver, CO 80225

National Weather Service
National Meteorological Center
W321, WWB, Room 201
ATTN: Mr. Quiroz
Washington, DC 20233

Mil Assistant for Atmos Sciences
Ofc of the Undersecretary of Defense
for Rsch & Engr/E&LS - Room 3D129
The Pentagon
Washington, DC 20301

Defense Communications Agency
Technical Library Center
Code 205
Washington, DC 20305

Director
Defense Nuclear Agency
ATTN: Technical Library
Washington, DC 20305

HQDA (DAEN-RDM/Dr. de Percin)
Washington, DC 20314

Director
Naval Research Laboratory
Code 5530
Washington, DC 20375

Commanding Officer
Naval Research Laboratory
Code 2627
Washington, DC 20375

Dr. J. M. MacCallum
Naval Research Laboratory
Code 1409
Washington, DC 20375

The Library of Congress
ATTN: Exchange & Gift Div
Washington, DC 20540
2

Head, Atmos Rsch Section
Div Atmospheric Science
National Science Foundation
1800 G. Street, NW
Washington, DC 20550

CPT Hugh Albers, Exec Sec
Interdept Committee on Atmos Science
National Science Foundation
Washington, DC 20550

Director, Systems R&D Service
Federal Aviation Administration
ATTN: ARD-54
2100 Second Street, SW
Washington, DC 20590

ADTC/DLODL
Eglin AFB, FL 32542

Naval Training Equipment Center
ATTN: Technical Library
Orlando, FL 32813

Det 11, 2WS/OI
ATTN: Maj Orondorff
Patrick AFB, FL 32925

USAFETAC/CB
Scott AFB, IL 62225

HQ, ESD/TOSI/S-22
Hanscom AFB, MA 01731

Air Force Geophysics Laboratory
ATTN: LCB (A. S. Carten, Jr.)
Hanscom AFB, MA 01731

Air Force Geophysics Laboratory
ATTN: LYD
Hanscom AFB, MA 01731

Meteorology Division
AFGL/LY
Hanscom AFB, MA 01731

US Army Liaison Office
MIT-Lincoln Lab, Library A-082
PO Box 73
Lexington, MA 02173

Director
US Army Ballistic Rsch Lab
ATTN: DRDAR-BLB (Dr. G. E. Keller)
Aberdeen Proving Ground, MD 21005

Commander
US Army Ballistic Rsch Lab
ATTN: DRDAR-BLP
Aberdeen Proving Ground, MD 21005

Director
US Army Armament R&D Command
Chemical Systems Laboratory
ATTN: DRDAR-CLJ-I
Aberdeen Proving Ground, MD 21010

Chief CB Detection & Alarms Div
Chemical Systems Laboratory
ATTN: DRDAR-CLC-CR (H. Tannenbaum)
Aberdeen Proving Ground, MD 21010

Commander
Harry Diamond Laboratories
ATTN: DELHD-CO
2800 Powder Mill Road
Adelphi, MD 20783

Commander
ERADCOM
ATTN: DRDEL-AP
2800 Powder Mill Road
Adelphi, MD 20783
2

Commander
ERADCOM
ATTN: DRDEL-CG/DRDEL-DC/DRDEL-CS
2800 Powder Mill Road
Adelphi, MD 20783

Commander
ERADCOM
ATTN: DRDEL-CT
2800 Powder Mill Road
Adelphi, MD 20783

Commander
ERADCOM
ATTN: DRDEL-EA
2800 Powder Mill Road
Adelphi, MD 20783

Commander
ERADCOM
ATTN: DRDEL-PA/DRDEL-ILS/DRDEL-E
2800 Powder Mill Road
Adelphi, MD 20783

Commander
ERADCOM
ATTN: DRDEL-PAO (S. Kimmel)
2800 Powder Mill Road
Adelphi, MD 20783

Chief
Intelligence Materiel Dev & Support Ofc
ATTN: DELEW-WL-I
Bldg 4554
Fort George G. Meade, MD 20755

Acquisitions Section, IRDB-D823
Library & Info Service Div, NOAA
6009 Executive Blvd
Rockville, MD 20852

Naval Surface Weapons Center
White Oak Library
Silver Spring, MD 20910

The Environmental Research
Institute of MI
ATTN: IRIA Library
PO Box 8618
Ann Arbor, MI 48107

Mr. William A. Main
USDA Forest Service
1407 S. Harrison Road
East Lansing, MI 48823

Dr. A. D. Belmont
Research Division
PO Box 1249
Control Data Corp
Minneapolis, MN 55440

Director
Naval Oceanography & Meteorology
NSTL Station
Bay St Louis, MS 39529

Director
US Army Engr Waterways Experiment Sta
ATTN: Library
PO Box 631
Vicksburg, MS 39180

Environmental Protection Agency
Meteorology Laboratory
Research Triangle Park, NC 27711

US Army Research Office
ATTN: DRXRO-PP
PO Box 12211
Research Triangle Park, NC 27709

Commanding Officer
US Army Armament R&D Command
ATTN: DRDAR-TSS Bldg 59
Dover, NJ 07801

Commander
HQ, US Army Avionics R&D Activity
ATTN: DAVAA-O
Fort Monmouth, NJ 07703

Commander/Director
US Army Combat Surveillance & Target
Acquisition Laboratory
ATTN: DELCS-D
Fort Monmouth, NJ 07703

Commander
US Army Electronics R&D Command
ATTN: DELCS-S
Fort Monmouth, NJ 07703

US Army Materiel Systems
Analysis Activity
ATTN: DRXSY-MP
Aberdeen Proving Ground, MD 21005

Director
US Army Electronics Technology &
Devices Laboratory
ATTN: DELET-D
Fort Monmouth, NJ 07703

Commander
US Army Electronic Warfare Laboratory
ATTN: DELEW-D
Fort Monmouth, NJ 07703

Commander
US Army Night Vision &
Electro-Optics Laboratory
ATTN: DELNV-L (Dr. Rudolf Buser)
Fort Monmouth, NJ 07703

Commander
ERADCOM Technical Support Activity
ATTN: DELSD-L
Fort Monmouth, NJ 07703

Project Manager, FIREFINDER
ATTN: DRCPM-FF
Fort Monmouth, NJ 07703

Project Manager, REMBASS
ATTN: DRCPM-RBS
Fort Monmouth, NJ 07703

Commander
US Army Satellite Comm Agency
ATTN: DRCPM-SC-3
Fort Monmouth, NJ 07703

Commander
ERADCOM Scientific Advisor
ATTN: DRDEL-SA
Fort Monmouth, NJ 07703

6585 TG/WE
Holloman AFB, NM 88330

AFWL/WE
Kirtland, AFB, NM 87117

AFWL/Technical Library (SUL)
Kirtland AFB, NM 87117

Commander
US Army Test & Evaluation Command
ATTN: STEWS-AD-L
White Sands Missile Range, NM 88002

Rome Air Development Center
ATTN: Documents Library
TSLD (Bette Smith)
Griffiss AFB, NY 13441

Commander
US Army Tropic Test Center
ATTN: STETC-TD (Info Center)
APO New York 09827

Commandant
US Army Field Artillery School
ATTN: ATSF-CD-R (Mr. Farmer)
Fort Sill, OK 73503

Commandant
US Army Field Artillery School
ATTN: ATSF-CF-R
Fort Sill, OK 73503

Director CFD
US Army Field Artillery School
ATTN: Met Division
Fort Sill, OK 73503

Commandant
US Army Field Artillery School
ATTN: Morris Swett Library
Fort Sill, OK 73503

Commander
US Army Dugway Proving Ground
ATTN: MT-DA-L
Dugway, UT 84022

Dr. C. R. Sreedrahan
Research Associates
Utah State University, UNC 48
Logan, UT 84322

Inge Dirmhirn, Professor
Utah State University, UNC 48
Logan, UT 84322

Defense Documentation Center
ATTN: DDC-TCA
Cameron Station Bldg 5
Alexandria, VA 22314
12

Commanding Officer
US Army Foreign Sci & Tech Center
ATTN: DRXST-1S1
220 7th Street, NE
Charlottesville, VA 22901

Naval Surface Weapons Center
Code G65
Dahlgren, VA 22448

Commander
US Army Night Vision
& Electro-Optics Lab
ATTN: DELNV-D
Fort Belvoir, VA 22060

Commander and Director
US Army Engineer Topographic Lab
ETL-TD-MB
Fort Belvoir, VA 22060

Director
Applied Technology Lab
DAVDL-EU-TSD
ATTN: Technical Library
Fort Eustis, VA 23604

Department of the Air Force
OL-C, 5WW
Fort Monroe, VA 23651

Department of the Air Force
5WW/DN
Langley AFB, VA 23665

Director
Development Center MCDEC
ATTN: Firepower Division
Quantico, VA 22134

US Army Nuclear & Chemical Agency
ATTN: MONA-WE
Springfield, VA 22150

Director
US Army Signals Warfare Laboratory
ATTN: DELSW-OS (Dr. R. Burkhardt)
Vint Hill Farms Station
Warrenton, VA 22186

Commander
US Army Cold Regions Test Center
ATTN: STECR-OP-PM
APO Seattle, WA 98733

Dr. John L. Walsh
Code 5560
Navy Research Lab
Washington, DC 20375

Commander
TRASANA
ATTN: ATAA-PL
(Dolores Anguiano)
White Sands Missile Range, NM 88002

Commander
US Army Dugway Proving Ground
ATTN: STEDP-MT-DA-M (Mr. Paul Carlson)
Dugway, UT 84022

Commander
US Army Dugway Proving Ground
ATTN: STEDP-MT-DA-T
(Mr. William Peterson)
Dugway, UT 84022

Commander
USATRADOC
ATTN: ATCD-SIE
Fort Monroe, VA 23651

Commander
USATRADOC
ATTN: ATCD-CF
Fort Monroe, VA 23651

Commander
USATRADOC
ATTN: Tech Library
Fort Monroe, VA 23651

ATMOSPHERIC SCIENCES RESEARCH PAPERS

1. Lindberg, J.D., "An Improvement to a Method for Measuring the Absorption Coefficient of Atmospheric Dust and other Strongly Absorbing Powders, " ECOM-5565, July 1975.
2. Avara, Elton, P., "Mesoscale Wind Shears Derived from Thermal Winds," ECOM-5566, July 1975.
3. Gomez, Richard B., and Joseph H. Pierluissi, "Incomplete Gamma Function Approximation for King's Strong-Line Transmittance Model," ECOM-5567, July 1975.
4. Blanco, A.J., and B.F. Engebos, "Ballistic Wind Weighting Functions for Tank Projectiles," ECOM-5568, August 1975.
5. Taylor, Fredrick J., Jack Smith, and Thomas H. Pries, "Crosswind Measurements through Pattern Recognition Techniques," ECOM-5569, July 1975.
6. Walters, D.L., "Crosswind Weighting Functions for Direct-Fire Projectiles," ECOM-5570, August 1975.
7. Duncan, Louis D., "An Improved Algorithm for the Iterated Minimal Information Solution for Remote Sounding of Temperature," ECOM-5571, August 1975.
8. Robbiani, Raymond L., "Tactical Field Demonstration of Mobile Weather Radar Set AN/TPS-41 at Fort Rucker, Alabama," ECOM-5572, August 1975.
9. Miers, B., G. Blackman, D. Langer, and N. Lorimier, "Analysis of SMS/GOES Film Data," ECOM-5573, September 1975.
10. Manquero, Carlos, Louis Duncan, and Rufus Bruce, "An Indication from Satellite Measurements of Atmospheric CO2 Variability," ECOM-5574, September 1975.
11. Petracca, Carmine, and James D. Lindberg, "Installation and Operation of an Atmospheric Particulate Collector," ECOM-5575, September 1975.
12. Avara, Elton P., and George Alexander, "Empirical Investigation of Three Iterative Methods for Inverting the Radiative Transfer Equation," ECOM-5576, October 1975.
13. Alexander, George D., "A Digital Data Acquisition Interface for the SMS Direct Readout Ground Station — Concept and Preliminary Design," ECOM-5577, October 1975.
14. Cantor, Israel, "Enhancement of Point Source Thermal Radiation Under Clouds in a Nonattenuating Medium," ECOM-5578, October 1975.
15. Norton, Colburn, and Glenn Hoidale, "The Diurnal Variation of Mixing Height by Month over White Sands Missile Range, N.M," ECOM-5579, November 1975.
16. Avara, Elton P., "On the Spectrum Analysis of Binary Data," ECOM-5580, November 1975.
17. Taylor, Fredrick J., Thomas H. Pries, and Chao-Huan Huang, "Optimal Wind Velocity Estimation," ECOM-5581, December 1975.
18. Avara, Elton P., "Some Effects of Autocorrelated and Cross-Correlated Noise on the Analysis of Variance, " ECOM-5582, December 1975.
19. Gillespie, Patti S., R.L. Armstrong, and Kenneth O. White, "The Spectral Characteristics and Atmospheric CO2 Absorption of the Ho^{+3}:YLF Laser at 2.05μm," ECOM-5583, December 1975.
20. Novlan, David J. "An Empirical Method of Forecasting Thunderstorms for the White Sands Missile Range," ECOM-5584, February 1976.
21. Avara, Elton P., "Randomization Effects in Hypothesis Testing with Autocorrelated Noise," ECOM-5585, February 1976.
22. Watkins, Wendell R., "Improvements in Long Path Absorption Cell Measurement," ECOM-5586, March 1976.
23. Thomas, Joe, George D. Alexander, and Marvin Dubbin, "SATTEL — An Army Dedicated Meteorological Telemetry System," ECOM-5587. March 1976.
24. Kennedy, Bruce W., and Delbert Bynum, "Army User Test Program for the RDT&E-XM-75 Meteorological Rocket," ECOM-5588, April 1976.

25. Barnett, Kenneth M., "A Description of the Artillery Meteorological Comparisons at White Sands Missle Range, October 1974 - December 1974 ('PASS' - Prototype Artillery [Meteorological] Subsystem)," ECOM-5589, April 1976.
26. Miller, Walter B., "Preliminary Analysis of Fall-of-Shot From Project 'PASS'," ECOM-5590, April 1976.
27. Avara, Elton P., "Error Analysis of Minimum Information and Smith's Direct Methods for Inverting the Radiative Transfer Equation," ECOM-5591, April 1976.
28. Yee, Young P., James D. Horn, and George Alexander, "Synoptic Thermal Wind Calculations from Radiosonde Observations Over the Southwestern United States," ECOM-5592, May 1976.
29. Duncan, Louis D., and Mary Ann Seagraves, "Applications of Empirical Corrections to NOAA-4 VTPR Observations," ECOM-5593, May 1976.
30. Miers, Bruce T., and Steve Weaver, "Applications of Meterological Satellite Data to Weather Sensitive Army Operations,"ECOM-5594, May 1976.
31. Sharenow, Moses, "Redesign and Improvement of Balloon ML-566," ECOM-5595, June, 1976.
32. Hansen, Frank V., "The Depth of the Surface Boundary Layer," ECOM-5596, June 1976.
33. Pinnick, R.G., and E.B. Stenmark, "Response Calculations for a Commercial Light-Scattering Aerosol Counter," ECOM-5597, July 1976.
34. Mason, J., and G.B. Hoidale, "Visibility as an Estimator of Infrared Transmittance," ECOM-5598, July 1976.
35. Bruce, Rufus E., Louis D. Duncan, and Joseph H. Pierluissi, "Experimental Study of the Relationship Between Radiosonde Temperatures and Radiometric-Area Temperatures," ECOM-5599, August 1976.
36. Duncan, Louis D., "Stratospheric Wind Shear Computed from Satellite Thermal Sounder Measurements," ECOM-5800, September 1976.
37. Taylor, F., P. Mohan, P. Joseph and T. Pries, "An All Digital Automated Wind Measurement System," ECOM-5801, September 1976.
38. Bruce, Charles, "Development of Spectrophones for CW and Pulsed Radiation Sources," ECOM-5802, September 1976.
39. Duncan, Louis D., and Mary Ann Seagraves,"Another Method for Estimating Clear Column Radiances," ECOM-5803, October 1976.
40. Blanco, Abel J., and Larry E. Taylor, "Artillery Meteorological Analysis of Project Pass," ECOM-5804, October 1976.
41. Miller, Walter, and Bernard Engebos," A Mathematical Structure for Refinement of Sound Ranging Estimates," ECOM-5805, November, 1976.
42. Gillespie, James B., and James D. Lindberg, "A Method to Obtain Diffuse Reflectance Measurements from 1.0 to 3.0 μm Using a Cary 17I Spectrophotometer," ECOM-5806, November 1976.
43. Rubio, Roberto, and Robert O. Olsen,"A Study of the Effects of Temperature Variations on Radio Wave Absorption,"ECOM-5807, November 1976.
44. Ballard, Harold N., "Temperature Measurements in the Stratosphere from Balloon-Borne Instrument Platforms, 1968-1975," ECOM-5808, December 1976.
45. Monahan, H.H., "An Approach to the Short-Range Prediction of Early Morning Radiation Fog," ECOM-5809, January 1977.
46. Engebos, Bernard Francis, "Introduction to Multiple State Multiple Action Decision Theory and Its Relation to Mixing Structures," ECOM-5810, January 1977.
47. Low, Richard D.H.,"Effects of Cloud Particles on Remote Sensing from Space in the 10-Micrometer Infrared Region," ECOM-5811, January 1977.
48. Bonner, Robert S., and R. Newton, "Application of the AN/GVS-5 Laser Rangefinder to Cloud Base Height Measurements," ECOM-5812, February 1977.
49. Rubio, Roberto, "Lidar Detection of Subvisible Reentry Vehicle Erosive Atmospheric Material," ECOM-5813, March 1977.
50. Low, Richard D.H., and J.D. Horn, "Mesoscale Determination of Cloud-Top Height: Problems and Solutions," ECOM-5814, March 1977.

51. Duncan, Louis D., and Mary Ann Seagraves, "Evaluation of the NOAA-4 VTPR Thermal Winds for Nuclear Fallout Predictions," ECOM-5815, March 1977.
52. Randhawa, Jagir S., M. Izquierdo, Carlos McDonald and Zvi Salpeter, "Stratospheric Ozone Density as Measured by a Chemiluminescent Sensor During the Stratcom VI-A Flight," ECOM-5816, April 1977.
53. Rubio, Roberto, and Mike Izquierdo, "Measurements of Net Atmospheric Irradiance in the 0.7- to 2.8-Micrometer Infrared Region," ECOM-5817, May 1977.
54. Ballard, Harold N., Jose M. Serna, and Frank P. Hudson Consultant for Chemical Kinetics, "Calculation of Selected Atmospheric Composition Parameters for the Mid-Latitude, September Stratosphere," ECOM-5818, May 1977.
55. Mitchell, J.D., R.S. Sagar, and R.O. Olsen, "Positive Ions in the Middle Atmosphere During Sunrise Conditions," ECOM-5819, May 1977.
56. White, Kenneth O., Wendell R. Watkins, Stuart A. Schleusener, and Ronald L. Johnson, "Solid-State Laser Wavelength Identification Using a Reference Absorber," ECOM-5820, June 1977.
57. Watkins, Wendell R., and Richard G. Dixon, "Automation of Long-Path Absorption Cell Measurements," ECOM-5821, June 1977.
58. Taylor, S.E., J.M. Davis, and J.B. Mason, "Analysis of Observed Soil Skin Moisture Effects on Reflectance," ECOM-5822, June 1977.
59. Duncan, Louis D. and Mary Ann Seagraves, "Fallout Predictions Computed from Satellite Derived Winds," ECOM-5823, June 1977.
60. Snider, D.E., D.G. Murcray, F.H. Murcray, and W.J. Williams, "Investigation of High-Altitude Enhanced Infrared Backround Emissions" (U), SECRET, ECOM-5824, June 1977.
61. Dubbin, Marvin H. and Dennis Hall, "Synchronous Meteorlogical Satellite Direct Readout Ground System Digital Video Electronics," ECOM-5825, June 1977.
62. Miller, W., and B. Engebos, "A Preliminary Analysis of Two Sound Ranging Algorithms," ECOM-5826, July 1977.
63. Kennedy, Bruce W., and James K. Luers, "Ballistic Sphere Techniques for Measuring Atomspheric Parameters," ECOM-5827, July 1977.
64. Duncan, Louis D., "Zenith Angle Variation of Satellite Thermal Sounder Measurements," ECOM-5828, August 1977.
65. Hansen, Frank V., "The Critical Richardson Number," ECOM-5829, September 1977.
66. Ballard, Harold N., and Frank P. Hudson (Compilers), "Stratospheric Composition Balloon-Borne Experiment," ECOM-5830, October 1977.
67. Barr, William C., and Arnold C. Peterson, "Wind Measuring Accuracy Test of Meteorological Systems," ECOM-5831, November 1977.
68. Ethridge, G.A. and F.V. Hansen, "Atmospheric Diffusion: Similarity Theory and Empirical Derivations for Use in Boundary Layer Diffusion Problems," ECOM-5832, November 1977.
69. Low, Richard D.H., "The Internal Cloud Radiation Field and a Technique for Determining Cloud Blackness," ECOM-5833, December 1977.
70. Watkins, Wendell R., Kenneth O. White, Charles W. Bruce, Donald L. Walters, and James D. Lindberg, "Measurements Required for Prediction of High Energy Laser Transmission," ECOM-5834, December 1977.
71. Rubio, Robert, "Investigation of Abrupt Decreases in Atmospherically Backscattered Laser Energy," ECOM-5835, December 1977.
72. Monahan, H.H. and R.M. Cionco, "An Interpretative Review of Existing Capabilities for Measuring and Forecasting Selected Weather Variables (Emphasizing Remote Means)," ASL-TR-0001, January 1978.
73. Heaps, Melvin G., "The 1979 Solar Eclipse and Validation of D-Region Models," ASL-TR-0002. March 1978.

74. Jennings, S.G., and J.B. Gillespie, "M.I.E. Theory Sensitivity Studies - The Effects of Aerosol Complex Refractive Index and Size Distribution Variations on Extinction and Absorption Coefficients Part II: Analysis of the Computational Results," ASL-TR-0003, March 1978.
75. White, Kenneth O. et al, "Water Vapor Continuum Absorption in the 3.5μm to 4.0μm Region," ASL-TR-0004, March 1978.
76. Olsen, Robert O., and Bruce W. Kennedy, "ABRES Pretest Atmospheric Measurements," ASL-TR-0005, April 1978.
77. Ballard, Harold N., Jose M. Serna, and Frank P. Hudson, "Calculation of Atmospheric Composition in the High Latitude September Stratosphere," ASL-TR-0006, May 1978.
78. Watkins, Wendell R. et al, "Water Vapor Absorption Coefficients at HF Laser Wavelengths," ASL-TR-0007, May 1978.
79. Hansen, Frank V., "The Growth and Prediction of Nocturnal Inversions," ASL-TR-0008, May 1978.
80. Samuel, Christine, Charles Bruce, and Ralph Brewer, "Spectrophone Analysis of Gas Samples Obtained at Field Site," ASL-TR-0009, June 1978.
81. Pinnick, R.G. et al., "Vertical Structure in Atmospheric Fog and Haze and its Effects on IR Extinction," ASL-TR-0010, July 1978.
82. Low, Richard D.H., Louis D. Duncan, and Richard B. Gomez, "The Microphysical Basis of Fog Optical Characterization," ASL-TR-0011, August 1978.
83. Heaps, Melvin G., "The Effect of a Solar Proton Event on the Minor Neutral Constituents of the Summer Polar Mesosphere," ASL-TR-0012, August 1978.
84. Mason, James B., "Light Attenuation in Falling Snow," ASL-TR-0013, August 1978.
85. Blanco, Abel J., "Long-Range Artillery Sound Ranging: "PASS" Meteorological Application," ASL-TR-0014, September 1978.
86. Heaps, M.G., and F.E. Niles, "Modeling the Ion Chemistry of the D-Region: A case Study Based Upon the 1966 Total Solar Eclipse," ASL-TR-0015, September 1978.
87. Jennings, S.G., and R.G. Pinnick, "Effects of Particulate Complex Refractive Index and Particle Size Distribution Variations on Atmospheric Extinction and Absorption for Visible Through Middle-Infrared Wavelengths," ASL-TR-0016, September 1978.
88. Watkins, Wendell R., Kenneth O. White, Lanny R. Bower, and Brian Z. Sojka, " Pressure Dependence of the Water Vapor Continuum Absorption in the 3.5- to 4.0-Micrometer Region," ASL-TR-0017, September 1978.
89. Miller, W.B., and B.F. Engebos, "Behavior of Four Sound Ranging Techniques in an Idealized Physical Enviroment," ASL-TR-0018, September 1978.
90. Gomez, Richard G., "Effectiveness Studies of the CBU-88/B Bomb, Cluster, Smoke Weapon" (U), CONFIDENTIAL ASL-TR-0019, September 1978.
91. Miller, August, Richard C. Shirkey, and Mary Ann Seagraves, "Calculation of Thermal Emission from Aerosols Using the Doubling Technique," ASL-TR-0020, November, 1978.
92. Lindberg, James D. et al., "Measured Effects of Battlefield Dust and Smoke on Visible, Infrared, and Millimeter Wavelengths Propagation: A Preliminary Report on Dusty Infrared Test-I (DIRT-I)," ASL-TR-0021, January 1979.
93. Kennedy, Bruce W., Arthur Kinghorn, and B.R. Hixon, "Engineering Flight Tests of Range Meteorological Sounding System Radiosonde," ASL-TR-0022, February 1979.
94. Rubio, Roberto, and Don Hoock, "Microwave Effective Earth Radius Factor Variability at Wiesbaden and Balboa," ASL-TR-0023, February 1979.
95. Low, Richard D.H., "A Theoretical Investigation of Cloud/Fog Optical Properties and Their Spectral Correlations," ASL-TR-0024, February 1979.

96. Pinnick, R.G., and H.J. Auvermann, "Response Characteristics of Knollenberg Light-Scattering Aerosol Counters," ASL-TR-0025, February 1979.
97. Heaps, Melvin G., Robert O. Olsen, and Warren W. Berning, "Solar Eclipse 1979, Atmospheric Sciences Laboratory Program Overview," ASL-TR-0026 February 1979.
98. Blanco, Abel J., "Long-Range Artillery Sound Ranging: 'PASS' GR-8 Sound Ranging Data," ASL-TR-0027, March 1979.
99. Kennedy, Bruce W., and Jose M. Serna, "Meteorological Rocket Network System Reliability," ASL-TR-0028, March 1979.
100. Swingle, Donald M., "Effects of Arrival Time Errors in Weighted Range Equation Solutions for Linear Base Sound Ranging," ASL-TR-0029, April 1979.
101. Umstead, Robert K., Ricardo Pena, and Frank V. Hansen, "KWIK: An Algorithm for Calculating Munition Expenditures for Smoke Screening/Obscuration in Tactical Situations," ASL-TR-0030, April 1979.
102. D'Arcy, Edward M., "Accuracy Validation of the Modified Nike Hercules Radar," ASL-TR-0031, May 1979.
103. Rodriguez, Ruben, "Evaluation of the Passive Remote Crosswind Sensor," ASL-TR-0032, May 1979.
104. Barber, T.L., and R. Rodriguez, "Transit Time Lidar Measurement of Near-Surface Winds in the Atmosphere," ASL-TR-0033, May 1979.
105. Low, Richard D.H., Louis D. Duncan, and Y.Y. Roger R. Hsiao, "Microphysical and Optical Properties of California Coastal Fogs at Fort Ord," ASL-TR-0034, June 1979.
106. Rodriguez, Ruben, and William J. Vechione, "Evaluation of the Saturation Resistant Crosswind Sensor," ASL-TR-0035, July 1979
107. Ohmstede, William D., "The Dynamics of Material Layers," ASL-TR-0036, July 1979.

★ U.S.GOVERNMENT PRINTING OFFICE: 1979 — 677-017/19